ELSEVIER

www.elsevier.nl/locate/jorganchem

Journal of Organometallic Chemistry 611 (2000) 314–322

Journal of Organometallic Chemistry

Synthesis and structures of bis(silylene)iron complexes containing new six-membered chelate rings

Hiromi Tobita *[1], Takahiro Sato, Masaaki Okazaki, Hiroshi Ogino *[2]

Department of Chemistry, Graduate School of Science, Tohoku University, Sendai 980-8578, Japan

Received 1 March 2000; accepted 20 March 2000

Abstract

Reaction of $Cp'Fe(CO)_2SiMe_2SiMe_2Cl$ (**1a**: $Cp' = \eta^5$-C_5H_5 (Cp), **1b**: $Cp' = \eta^5$-C_5Me_5 (Cp*)) with acetic acid in the presence of base (pyridine or Et_3N) afforded $Cp'Fe(CO)_2SiMe_2SiMe_2OCOMe$ (**2a**: $Cp' = Cp$, 77%; **2b**: $Cp' = Cp^*$, 87%). Similarly, the reaction of **1b** with 2-pyridone in the presence of Et_3N gave $Cp^*Fe(CO)_2SiMe_2SiMe_2O(2\text{-}C_5H_4N)$ (**3**, 43%). Photolysis of **2a**, **2b**, and **3** produced $Cp'(CO)Fe\{SiMe_2\cdots OC(Me)O\cdots SiMe_2\}$ (**4a**: $Cp' = Cp$, **4b**: $Cp' = Cp^*$) and $Cp^*(CO)Fe\{SiMe_2\cdots O(2\text{-}C_5H_4N)\cdots SiMe_2\}$ (**5**) quantitatively, in which an acetoxy or 2-pyridyloxy group bridges two silylene ligands to form a six-membered chelate ring. **4a** and **5** were structurally characterized by single-crystal X-ray diffraction experiments. All the Fe–Si bonds are significantly shorter than normal Fe–Si single bonds and are consistent with their unsaturated bond character. The six-membered chelate ring consists of two entirely different and delocalized unsaturated bond systems. © 2000 Elsevier Science S.A. All rights reserved.

Keywords: Silylene complex; Iron complex; Chelate; Photolysis; X-ray structure analysis

1. Introduction

Silylene complexes have attracted much attention not only as the analogs of carbene complexes having a transition metal–main group element unsaturated bond but also as intermediates in various transition-metal-mediated transformation reactions of organosilicon compounds [1]. In particular, silyl(silylene) complexes are considered to play important roles as intermediates in dehydrogenative silane coupling and scrambling of substituents on silanes catalyzed by late transition metal complexes [2]. A plausible mechanism for the dehydrogenative silane coupling and scrambling of substituents on silanes through silyl(silylene) complexes is illustrated in Scheme 1. Key processes are reversible 1,2-silyl-migration and 1,3-R-migration on silyl(silylene) complexes. The existence of these processes is supported by a number of observations mentioned in the next paragraph, and also by several intriguing reactions of transition metal complexes with silanes [3] and germanes [4].

Pannell et al. [5] and we [6] first suggested the formation of silyl(silylene) complexes via 1,2-silyl-migration and the scrambling of substituents on silicon via 1,3-R-migration to explain the photochemical behavior of disilanyl(carbonyl)iron complexes. Then we succeeded in isolating and characterizing the 1,2-silyl-migration products, i.e. alkoxy- or amino-bridged bis(silylene) complexes having a four-membered chelate ring (Type A) of Fe [7], Ru [8], Mn [9], Cr, Mo, and W [10] and Ir [11], alkoxy-stabilized disilanyl(silylene) complexes

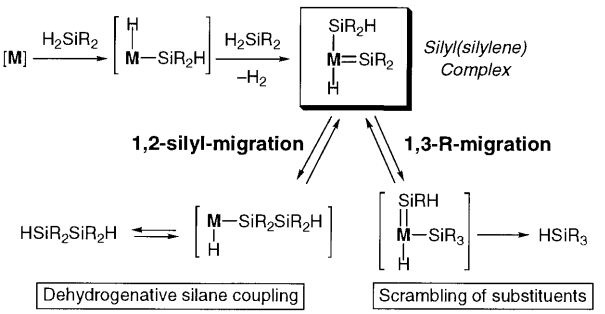

Scheme 1.

[1] *Corresponding author. Fax: +81-22-217-6543; e-mail: tobita@inorg.chem.tohoku.ac.jp (H. Tobita)

[2] *Corresponding author.

PII: S0022-328X(00)00494-0

(Type B) of Fe and Ru [12], and external-donor-stabilized silyl(silylene) complexes (Type C) of Fe [13] and W [14]. More recently, we succeeded in the synthesis and structure determination of a donor-free germyl(germylene)tungsten complex via an analogous 1,2-germyl-migration [15]. This is indisputable evidence for the facile 1,2-silyl-migration. With regard to the 1,3-R-migration, Pannell reported various redistribution reactions of polysilanyliron complexes which can be reasonably explained by postulating this process in combination with the 1,2-silyl-migration [16]. 1,3-R-Migration was also observed in the rearrangement reactions of the complexes of W [17], Fe [18], Rh [19], and Ni [20]. As more direct evidence for 1,3-R-migration, a fast exchange of methyl groups on the silyl and silylene ligands in the Type C complexes of Fe and W has been observed by variable temperature NMR spectroscopy [13,14]. We recently reviewed our researches on silyl(silylene) and bis(silylene) complexes focusing on the complexes of iron and ruthenium [21].

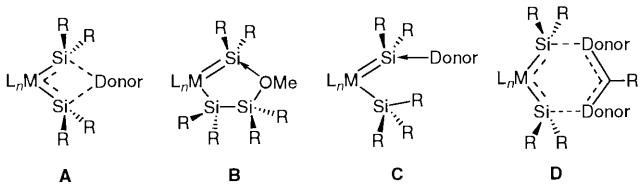

Most of known donor-free and donor-stabilized silylene complexes are extremely air- and moisture-sensitive due to the strong polarization of the metal–silicon bond in $M^{\delta-}=Si^{\delta+}$ fashion [22]. These types of complexes containing weak or reactive ligand–metal bonds can frequently be stabilized by including the bonds in a chelate ring. However, in the case of Type A complexes, the ring strain in the four-membered chelate ring and/or the coordination of only one donor atom to two silylene ligands may be destabilizing them. Therefore, we next tried to prepare the bis(silylene) complexes containing a less-strained six-membered chelate ring (Type D) in which two silylene ligands are separately coordinated to two donor atoms. In this paper, we report the synthesis, spectroscopic properties, and structure determinations of acetoxy- and 2-pyridyloxy-bridged bis(silylene)iron complexes.

2. Results and discussion

2.1. Synthesis of the precursors *2a*, *2b*, and *3*

Acetoxydisilanyl complexes **2a** and **2b** were prepared by applying a usual preparation method of silyl acetate such as $Me_3SiOCOMe$ [23]. Thus, the reactions of chlorodisilanyl complexes **1a** and **1b** with acetic acid in the presence of base afforded **2a** and **2b** in 77 and 87% yields, respectively (Eq. (1)).

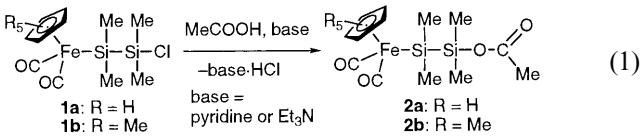

(1)

In a similar manner, the reaction of **1b** with 2-pyridone in the presence of Et_3N gave 2-pyridyloxydisilanyl complex **3** in 43% yield (Eq. (2)).

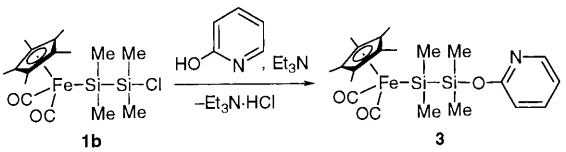

(2)

The ^{1}H- and ^{29}Si-NMR and IR spectral data of **2a**, **2b**, and **3** are summarized in Table 1. In the ^{29}Si-NMR spectra of **2a**, **2b**, and **3**, two signals appeared in the range of δ 10–25 ppm which are normal for disilanyliron complexes [7]. All the spectroscopic and analytical data for **2a**, **2b**, and **3** are consistent with the structures shown in Eqs. (1) and (2). These complexes are obtained as air- and moisture-sensitive yellow crystals and have to be handled under inert gas atmosphere.

2.2. Photolysis of *2a*, *2b*, *3* — synthesis of bis(silylene) complexes *4a*, *4b*, *5*

Irradiation of a C_6D_6 solution of **2a**, **2b**, or **3** resulted in clean conversion with gas evolution to a single product **4a**, **4b**, or **5**, respectively, which was observed by ^{1}H-NMR spectroscopy (Eqs. (3) and (4)). When these reactions were carried out on large scales in hexane or pentane solutions, the products precipitated out as yellow crystals during irradiation due to their relatively low solubility in these solvents.

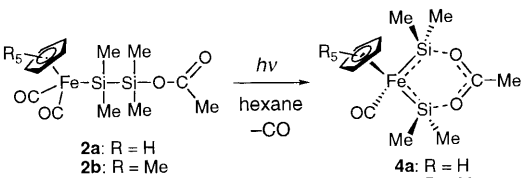

(3)

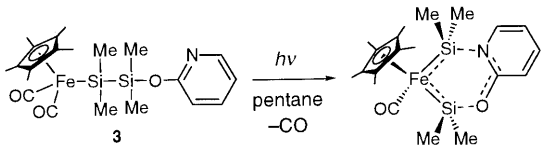

(4)

The ^{1}H- and ^{29}Si-NMR and IR spectral data of the products **4a**, **4b**, and **5** are summarized in Table 1. The ^{29}Si-NMR signals of the products appear at the field lower than 100 ppm. This downfield shift is typical of donor-stabilized silylene complexes [7–14]. Two silicon atoms are equivalent in **4a** and **4b** while they are

Table 1
The ^{1}H-, ^{29}Si-NMR and IR spectral data of acetoxy- and 2-pyridyloxy-substituted disilanyliron complexes **2a**, **2b**, **3** and their photolysis products **4a**, **4b**, **5**

Compound	^{1}H-NMR (C_6D_6) δ (ppm)	^{29}Si-NMR (C_6D_6) δ (ppm)	IR ν(C–O) (cm^{-1})
2a	0.51 (s, 6H, SiMe)	15.0	ν(CO) 1998 vs [a]
	0.61 (s, 6H, SiMe)	22.9	1947 vs
	1.74 (s, 3H, CH_3CO_2)		ν(OCO) 1718 s
	4.21 (s, 5H, Cp)		ν(SiOC) 1263 vs
2b	0.68 (s, 6H, SiMe)	13.3	ν(CO) 1971 vs [b]
	0.69 (s, 6H, SiMe)	24.5	1919 vs
	1.49 (s, 15H, Cp*)		ν(OCO) 1699 s
	1.84 (s, 3H, CH_3CO_2)		ν(SiOC) 1263 vs
3	0.74 (s, 6H, SiMe)	13.7	ν(CO) 1971 vs [b]
	0.83 (s, 6H, SiMe)	22.1	1921 vs
	1.55 (s, 15H, Cp*)		
	6.39–6.43 (m, 1H, aromatic)		
	6.65–6.68 (m, 1H, aromatic)		
	7.02–7.05 (m, 1H, aromatic)		
	8.08–8.10 (m, 1H, aromatic)		
4a	0.56 (s, 6H, SiMe)	122.9	ν(CO) 1875 vs [c]
	0.83 (s, 6H, SiMe)		ν(OCO) 1539 m
	1.33 (s, 3H, CH_3CO_2)		1470 s
	4.13 (s, 5H, Cp)		
4b	0.65 (s, 6H, SiMe)	126.6	ν(CO) 1867 vs [c]
	0.81 (s, 6H, SiMe)		ν(OCO) 1562 m
	1.38 (s, 3H, CH_3CO_2)		1470 s
	1.75 (s, 15H, Cp*)		
5	In toluene-d_8	In toluene-d_8	ν(CO) 1856 vs [b]
	0.61 (s, 3H, SiMe)	104.0	
	0.74 (s, 3H, SiMe)	112.2	
	0.81 (s, 3H, SiMe)		
	0.82 (s, 3H, SiMe)		
	1.83 (s, 15H, Cp*)		
	5.95–6.00 (m, 1H, aromatic)		
	6.29–6.32 (m, 1H, aromatic)		
	6.66–6.72 (m, 1H, aromatic)		
	7.57–7.59 (m, 1H, aromatic)		

[a] In hexane solution.
[b] KBr pellet.
[c] In C_6D_6 solution.

inequivalent in **5**. Each of the IR spectra of **4a**, **4b**, or **5** show only one CO stretching band assigned to a terminal carbonyl ligand in the range of 1850–1880 cm^{-1} which clearly signifies the loss of one CO ligand during the photoreaction. This is further supported by the mass spectra of the products which show the molecular ion peaks with the m/z values smaller by 28 (i.e. CO) than their precursors as base peaks. In the case of acetoxy derivatives **4a** and **4b**, two C–O stretching bands for an acetoxy group appeared close to each other with the separation of 69–92 cm^{-1}. This is characteristic of an acetato ligand coordinated through both oxygen atoms [24] and is in sharp contrast with the bands for an acetoxy group bonded through only one oxygen atom for which the separation is much larger (e.g. **2a**: 455 cm^{-1}, **2b**: 436 cm^{-1}). These spectroscopic features of **4a** and **4b** are consistent with the structures shown in Eq. (3), namely, the acetoxy-bridged bis(silylene)iron complexes having a six-membered chelate ring. A similar structure was also expected for **5** (Eq. (4)). The six-membered structures of **4a** and **5** were confirmed by the X-ray crystal structure analysis. Possible isomers of **4a**, **4b**, and **5** with four-membered chelate rings; i.e. **4a**′, **4b**′, and **5**′, were not observed in solution or in the solid state. Apparently, the bis(silylene) complexes favor the less strained structure (vide infra).

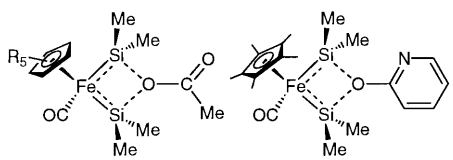

4a': R = H
4b': R = Me

5'

Table 2
Crystal data for Cp(CO)Fe{$SiMe_2$···OC(Me)O···$SiMe_2$} (**4a**)

Formula	$C_{12}H_{20}FeO_3Si_2$
Formula weight	324.31
Crystal size (mm)	$0.40\times0.35\times0.35$
Color of crystals	Yellow
Temperature (°C)	20
Crystal system	Monoclinic
Space group	$P2_1/a$
a (Å)	16.732(8)
b (Å)	11.65(2)
c (Å)	17.825(10)
β (°)	115.15(3)
V (Å^3)	3143(6)
Z	8
D_{calc} (g cm^{-3})	1.370
μ Mo–K_α (cm^{-1})	11.08
2θ Range (°)	3–55
Scan mode	ω–2θ
ω Scan width (°)	$1.00+0.35\tan\theta$
ω Scan rate (° min^{-1})	4.0
Number of unique data	7585 ($R_{int}=0.044$)
Number of data used with $I_o>3\sigma(I_o)$	2808
Number of parameters refined	325
R [a]	0.049
R_w [b]	0.073

[a] $R=\Sigma||F_o|-|F_c||/\Sigma|F_o|$.
[b] $R_w=[\Sigma\, w(|F_o|-|F_c|)^2/\Sigma\, w|F_o|^2]^{1/2}$; $w=[\sigma^2(|F_o|)+(p^2/4)F_o^2]^{-1}$, where $p=0.132$.

Table 3
Crystal data for Cp*(CO)Fe{$SiMe_2$···O(2-C_5H_4N)···$SiMe_2$} (**5**)

Empirical formula	$C_{20}H_{31}FeNO_2Si_2$
Formula weight	429.49
Crystal size (mm)	$0.5\times0.3\times0.15$
Color of crystals	Yellow
Temperature (°C)	20
Crystal system	Triclinic
Space group	$P\bar{1}$
a (Å)	8.8916(8)
b (Å)	16.5015(16)
c (Å)	8.2802(10)
α (°)	97.5383(18)
β (°)	110.682(5)
γ (°)	81.1359(12)
V (Å^3)	1119.2(2)
Z	2
D_{calc} (g cm^{-3})	1.274
Absorption coefficient (mm^{-1})	0.794
θ Range for data collection (°)	2.46–27.48
Reflections collected	9723
Independent reflections	4865 [$R_{int}=0.0378$]
Completeness to $\theta=27.48°$ (%)	94.3
Absorption correction	Integration
Max/min transmission	0.864896 and 0.739310
Data/restraints/parameters	4865/0/235
Final R indices [$I>2\sigma(I)$]	[a] $R_1=0.0496$, [b] $wR_2=0.1354$
R indices (all data)	$R_1=0.0568$, $wR_2=0.1445$

[a] $R_1=\Sigma||F_o|-|F_c||/\Sigma|F_o|$; $wR_2=[\Sigma[w(F_o^2-F_c^2)^2]/\Sigma[w(F_o^2)^2]]^{1/2}$
[b] $w=1/[\sigma^2(F_o^2)+(0.0754P)^2+0.7837P]$ where $P=(F_o^2+2F_c^2)/3$.

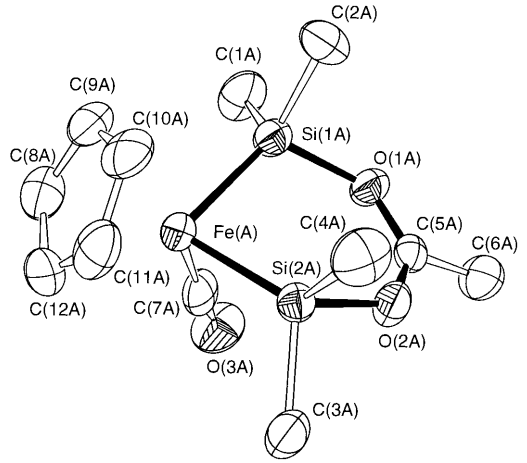

Fig. 1. ORTEP drawing of Cp(CO)Fe{$SiMe_2$···OC(Me)O···$SiMe_2$} (**4a**) with 50% thermal ellipsoids.

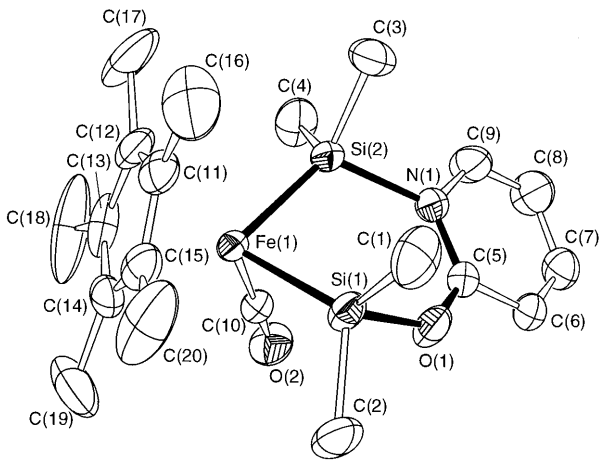

Fig. 2. ORTEP drawing of Cp*(CO)Fe{$SiMe_2$···O(2-C_5H_4N)···$SiMe_2$} (**5**) with 30% thermal ellipsoids.

2.3. Crystal structures of bis(silylene) complexes *4a* and *5*

Crystal data for **4a** and **5** are summarized in Tables 2 and 3, respectively. An asymmetric unit of the crystal of **4a** contains two crystallographically independent molecules A and B, which are nearly identical. ORTEP drawings of the molecule A of **4a** and **5** are depicted in Figs. 1 and 2, respectively. Both **4a** and **5** possess a six-membered chelate ring. A molecule of **4a** has an approximate mirror plane containing the centroid of the Cp ligand, a carbonyl ligand, and Fe, C(5), and C(6) and bisecting the six-membered chelate ring. Therefore, the lengths of the pairs of Fe–Si, Si–O, and O–C bonds in the chelate ring are almost the same, respectively. In the chelate ring, five atoms Si(1)–O(1)–C(5)–O(2)–Si(2) are nearly coplanar, but Fe deviates significantly from the plane: The dihedral angle between the planes defined by Si(1)–Fe–Si(2) and

Si(1)–O(1)–C(5)–O(2)–Si(2) is 143.37°. This bending of the chelate ring apparently results from the steric repulsion between the Cp ligand and the methyl groups on the silicon atoms: The shortest separation between them is 3.59(1) Å for C(4A)···C(10A) that is shorter than the sum of the van der Waals radii (3.7 Å). Similarly, in **5** the five atoms Si(1)–O(1)–C(5)–N(1)–Si(2) plus the atoms in the pyridine ring are almost in one plane although the planarity is worse than that in **4a**. Fe(1) deviates from this plane and the dihedral angle between the planes defined by Si(1)–Fe(1)–Si(2) and Si(1)–O(1)–C(5)–N(1)–Si(2) is 140.87(5)°.

Selected interatomic distances and bond angles of **4a** and **5** are listed in Tables 4 and 5, respectively. The Fe–Si bonds in **4a** (2.199(2)-2.206(3) Å) are shorter than the known Fe–Si single bonds having two methyl groups on the silicon atom (2.30–2.46 Å) [1] and also than the known Fe–Si unsaturated bonds having two methyl groups on the silicon atom (2.207–2.292 Å) [1]. These values suggest that both of the Fe–Si bonds bear significant unsaturated bond character. On the other hand, the Si–O bonds in **4a** (1.797(6)–1.825(6) Å) are much longer than normal Si–O single bonds (1.58–1.65 Å) [1,25] and are comparable to those of a four-membered bis(silylene)iron complexes, Cp*(CO)Fe{$SiMe_2$···OMe···SiMe(OMe)} (1.793(9), 1.799(8) A) [7a,b]. Evidently the Si–O bonds in **4a** have a significant dative bond character. The distances of the two C(5)–O bonds in the acetoxy group (molecule A: 1.262(9), 1.268(9) Å; molecule B: 1.257(9), 1.265(9) Å) are nearly equal and are in a normal range of didentate acetato ligands bridging two metal atoms (1.255–1.273 Å) [26]. These structural features demonstrate that two entirely different and delocalized unsaturated bond systems; i.e. Si(1)–Fe–Si(2) and O(1)–C(5)–O(2), exist in a six-membered chelate ring.

In **5**, the length of the Fe–Si bond directing toward the Si coordinated to N (2.2064(9) Å) is shorter than that directing toward the Si coordinated to O (2.2225(9) Å). Both of them are in any case shorter than the normal Fe–Si single bond. The Si–N bond (1.944(3) Å) and Si–O bond (1.750(2) Å) are both longer than the corresponding single bonds (normal Si–N single bonds: 1.70–1.76 Å) [25]. These data suggest that, although the unsaturated bonds delocalize over two three-atom linkages; i.e. Si(1)–Fe–Si(2) and O(1)–C(5)–N(1), the unsaturated bond character of the Fe–Si(2) bond is higher than that of Fe–Si(1).

Table 4
Selected interatomic distances (Å) and angles (°) for Cp(CO)Fe{$SiMe_2$···OC(Me)O···$SiMe_2$} (**4a**)

	Molecule A	Molecule B
Interatomic distances		
Fe–Si(1)	2.206(3)	2.204(3)
Fe–Si(2)	2.199(2)	2.204(3)
Fe–C(7)	1.73(1)	1.715(9)
Si(1)–O(1)	1.823(6)	1.797(6)
Si(2)–O(2)	1.805(6)	1.825(6)
Si(1)–C(1)	1.861(9)	1.87(1)
Si(1)–C(2)	1.88(1)	1.85(1)
Si(2)–C(3)	1.879(9)	1.86(1)
Si(2)–C(4)	1.87(1)	1.88(1)
O(1)–C(5)	1.262(9)	1.257(9)
O(2)–C(5)	1.268(9)	1.265(9)
O(3)–C(7)	1.16(1)	1.16(1)
C(5)–C(6)	1.47(1)	1.47(1)
Si(1)–Si(2)	3.050(3)	3.018(3)
Bond angles		
Si(1)–Fe–Si(2)	87.67(9)	86.4(1)
Si(1)–Fe–C(7)	86.2(3)	87.7(3)
Si(2)–Fe–C(7)	87.0(3)	87.3(3)
Fe–Si(1)–O(1)	113.8(2)	113.4(2)
Fe–Si(1)–C(1)	117.0(3)	116.5(4)
Fe–Si(1)–C(2)	121.4(3)	121.9(4)
O(1)–Si(1)–C(1)	95.2(4)	96.0(4)
O(1)–Si(1)–C(2)	99.0(4)	99.1(5)
C(1)–Si(1)–C(2)	106.1(5)	105.7(5)
Fe–Si(2)–O(2)	114.7(2)	113.3(2)
Fe–Si(2)–C(3)	117.5(3)	118.4(3)
Fe–Si(2)–C(4)	121.2(3)	121.3(3)
O(2)–Si(2)–C(3)	96.0(3)	95.3(4)
O(2)–Si(2)–C(4)	97.5(4)	99.4(4)
C(3)–Si(2)–C(4)	105.5(4)	104.8(5)
Si(1)–O(1)–C(5)	130.3(5)	130.6(5)
Si(2)–O(2)–C(5)	131.1(5)	129.6(5)
O(1)–C(5)–O(2)	124.4(7)	124.4(7)
O(1)–C(5)–C(6)	117.7(8)	117.2(7)
O(2)–C(5)–C(6)	117.8(7)	118.5(7)
Fe–C(7)–O(3)	176.3(8)	177.8(8)

Table 5
Selected interatomic distances (Å) and angles (°) for Cp*(CO)Fe{$SiMe_2$···O(2-C_5H_4N)···$SiMe_2$} (**5**)

Interatomic distances			
Fe(1)–Si(1)	2.2225(9)	Fe(1)–Si(2)	2.2064(9)
Fe(1)–C(10)	1.704(3)	Si(1)–O(1)	1.750(2)
Si(2)–N(1)	1.944(3)	Si(1)–C(1)	1.898(5)
Si(1)–C(2)	1.887(4)	Si(2)–C(3)	1.873(4)
Si(2)–C(4)	1.899(4)	O(1)–C(5)	1.290(4)
N(1)–C(5)	1.341(4)	O(2)–C(10)	1.172(4)
C(5)–C(6)	1.416(4)	C(6)–C(7)	1.346(5)
C(7)–C(8)	1.394(6)	C(8)–C(9)	1.343(6)
C(9)–N(1)	1.366(4)	Si(1)···Si(2)	3.021(1)
Bond angles			
Si(1)–Fe(1)–Si(2)	86.00(3)	Si(1)–Fe(1)–C(10)	86.73(10)
Si(2)–Fe(1)–C(10)	86.35(11)	Fe(1)–Si(1)–O(1)	113.05(9)
Fe(1)–Si(1)–C(1)	121.98(16)	Fe(1)–Si(1)–C(2)	118.22(17)
O(1)–Si(1)–C(1)	99.8(2)	O(1)–Si(1)–C(2)	94.26(16)
C(1)–Si(1)–C(2)	104.7(3)	Fe(1)–Si(2)–N(1)	116.21(8)
Fe(1)–Si(2)–C(3)	123.49(16)	Fe(1)–Si(2)–C(4)	113.14(17)
N(1)–Si(2)–C(3)	97.66(17)	N(1)–Si(2)–C(4)	96.74(18)
C(3)–Si(2)–C(4)	105.5(3)	Si(1)–O(1)–C(5)	133.8(2)
Si(2)–N(1)–C(5)	125.4(2)	O(1)–C(5)–N(1)	122.2(3)
Fe(1)–C(10)–O(2)	178.7(3)		

The sums of the bond angles between the three bonds except the dative bond around the Si atoms for **4a** (344.1–344.5°) and those for **5** (Si(1): 344.9°; Si(2): 342.1°) are between the sum of three valence angles around an ideal sp^2-hybridized atom (360°) and sp^3-hybridized atom (328.5°). This implies that there is some contribution of the π interaction between the sp^2-hybridized Si atoms and the iron center. A slightly larger pyramidalization of Si(2) may be attributable to the steric repulsion between the pyridine ring and the methyl groups on Si(2). The Si–Fe–Si angles are 87.67(9)° (molecule A) and 86.4(1) (molecule B) for **4a** and 86.00(3)° for **5**. These are much larger than the corresponding values of four-membered bis(silylene)-iron complexes, Cp*(CO)Fe{$SiMe_2$···OMe···SiMe(OMe)} (72.60(11)°) [7a,b] and Cp*(CO)Fe{$SiMe_2$···NEt_2···$SiMe_2$} (71.54(6), 71.78(5)°) [7c]. These data suggest that the ring in the six-membered chelate complexes **4a** and **5** is less strained than that in the four-membered possible isomers **4a′** and **5′**, and it causes the preference of the former over the latter. Accompanied by the widening of the Si–Fe–Si angles, the distances between two Si atoms in **4a** (3.050(3), 3.018(3) Å) and **5** (3.021(1) Å) become longer than those in Cp*(CO)Fe{$SiMe_2$···OMe···SiMe(OMe)} (2.622(4) Å) [7a,b] and Cp*(CO)Fe{$SiMe_2$···NEt_2···$SiMe_2$} (2.605(2), 2.613(2) Å) [7c].

2.4. Some considerations on the spectroscopic properties of bis(silylene) complexes

We reported previously that the fluxional behavior caused by the rotation of the germylene ligand in alkoxy-bridged bis(germylene)- and (germylene)-(silylene)iron complexes can be observed by VT-NMR spectroscopy [27]. In contrast, so far none of the known donor-bridged bis(silylene)iron complexes shows the analogous fluxional behavior through the rotation of the silylene ligand. We demonstrated that the easiness of the fluxional behavior of bis(silylene) complexes depends on the electron richness of the metal center [28]. Another factor which can determine the easiness of the fluxional behavior is the bridging donor group. Temperature dependence of the ^{1}H-NMR spectra of **4a** and **5** in toluene-d_8 was examined to estimate the effect of the bridging donor group. Although the signals showed some shift depending on temperature, no coalescence of the signals of Si–Me groups in **4a** and **5** was observed up to approximately 80°C. This clearly shows that the ability of acetoxy and 2-pyridyloxy groups to stabilize bis(silylene) complexes is at least comparable to alkoxy and amino groups.

Table 6
The ^{1}H-NMR chemical shifts for the acetoxy groups of **2a** and **4a** and their differences in several solvents

Solvent	δ (ppm)		$\Delta\delta$(**2a**–**4a**) (ppm)
	2a	**4a**	
Benzene-d_6	1.74	1.33	0.41
Toluene-d_8	1.76	1.44	0.32
Cyclohexane-d_{12}	1.94	2.11	−0.17
Acetonitrile-d_3	2.03	2.25	−0.22
Acetone-d_6	2.04	2.35	−0.31

One of characteristic spectroscopic properties of donor-bridged bis(silylene) complexes is a large upfield shift of the ^{1}H-NMR signal for a substituents on the bridging donor group. Especially, in the cases of methoxy-bridged bis(silylene) complexes, the ^{1}H-NMR signal of methoxy protons in benzene-d_6 always appears in the field higher than 3 ppm, and is upfield shifted by 0.45–0.8 ppm compared with that in the corresponding precursors; i.e. methoxydisilanyl complexes or $HSiMe_2SiMe_2OMe$ (3.27 ppm). An analogous upfield shift of the ^{1}H-NMR signal of the bridging acetoxy group in **4a** and **4b** was also observed in benzene-d_6: **4a**: 1.33 and **4b**: 1.38 ppm in comparison with **2a**: 1.75 and **2b**: 1.84 ppm. Interestingly, in ^{13}C-NMR spectra, no significant chemical shift difference for methoxy or acetoxy groups has been observed between known bis(silylene) complexes and their precursors; i.e. methoxydisilanyl complexes or $HSiMe_2SiMe_2OMe$.

In order to clarify the origin of the upfield shift, we compared the ^{1}H-NMR spectra of **2a** and **4a** measured in several solvents. Table 6 shows the ^{1}H-NMR chemical shifts for the acetoxy groups of **2a** and **4a** and their differences in several solvents. To our surprise, an upfield shift was observed only in aromatic solvents (benzene-d_6 and toluene-d_8), whereas in cyclohexane-d_{12}, acetonitrile-d_3, and acetone-d_6 a downfield shift was observed regardless of the polarity of the solvent. This phenomenon implies that the upfield shift of the acetoxy protons originates probably from the ring current effect of aromatic solvents specifically oriented by the interaction between the six-membered chelate ring in **4a** and the aromatic ring instead of the inherent electronic properties of the bis(silylene) complexes.

3. Experimental

All syntheses and chemical manipulations were carried out under nitrogen using either standard Schlenk tube or high vacuum techniques. Acetic acid was purified by adding acetic anhydride and distilling from CrO_3. 2-Pyridone was purified by sublimation. Pyridine was distilled from KOH and Et_3N was distilled from sodium. Ether and hexane were distilled from sodium-benzophenone prior to use. Hexane and pentane for

photolysis and benzene-d_6, toluene-d_8, and cyclohexane-d_{12} were trap-to-trap-transferred under high vacuum from potassium mirror. Acetonitrile-d_3 and acetone-d_6 were trap-to-trap-transferred under high vacuum from molecular sieves 3Å. $CpFe(CO)_2SiMe_2SiMe_2Cl$ (**1a**) [7b] and $Cp^*Fe(CO)_2SiMe_2SiMe_2Cl$ (**1b**) [7b] were prepared according to literature procedures. ^1H-, ^{13}C-, and ^{29}Si-NMR spectra were recorded on a Bruker ARX-300 spectrometer and referenced to $SiMe_4$. IR spectra were measured on a Horiba FT-200 spectrometer. Mass spectra were recorded on a Shimadzu GCMS-QP5050A mass spectrometer. Photolysis was performed with an Ushio UM-452 450 W medium-pressure Hg lamp placed in a water-cooled, quartz jacket. Sample solutions were irradiated in Pyrex tubes.

3.1. Synthesis of $CpFe(CO)_2SiMe_2SiMe_2OCOMe$ (2a)

Acetic acid (0.977 g, 16.3 mmol) in ether (50 ml) was added dropwise with vigorous stirring to a solution of $CpFe(CO)_2SiMe_2SiMe_2Cl$ (**1a**) (4.94 g, 15.0 mmol) and pyridine (1.32 g, 16.7 mmol) in ether (50 ml). After stirring for 2 h, the supernatant was separated by a cannula and the residual yellow powder was washed with hexane (20 ml × 3). Organic layers were combined and the solvent was removed under reduced pressure to give a yellow oily residue. Molecular distillation of the residue at 115°C/2.0×10^{-3} mmHg afforded **2a** (4.09 g, 11.6 mmol, 77%) as reddish orange crystals. Further purification by recrystallization from hexane gave yellow crystals of **2a**. $^{13}C\{^1H\}$-NMR (75.5 MHz, C_6D_6): δ 0.4 (SiMe), 3.4 (SiMe), 22.5 (CH_3CO_2), 83.3 (Cp), 171.6 (CH_3CO_2), 215.5 (FeCO). Mass spectrum (EI, 70 eV): m/z 337 ($M^+ - Me$, 1.1), 324 ($M^+ - CO$, 1.8), 282 (22), 254 (14), 236 (15), 207 ($M^+ - MeCO_2 - SiMe_2 - CO$, 4.9), 195 (4.2), 175 ($M^+ - CpFe(CO)_2$, 100), 133 (25), 121 ($CpFe^+$, 13), 117 ($M^+ - CpFe(CO)_2 - SiMe_2$, 18), 93 (11), 73 (27). Anal. Found: C, 44.38; H, 5.86. Calc. for $C_{13}H_{20}FeO_4Si_2$: C, 44.32; H, 5.72%.

3.2. Synthesis of $Cp^*Fe(CO)_2SiMe_2SiMe_2OCOMe$ (2b)

Acetic acid (135 mg, 2.25 mmol) and then Et_3N (214 mg, 2.11 mmol) was added by microsyringe with stirring to a solution of $Cp^*Fe(CO)_2SiMe_2SiMe_2Cl$ (**1b**) (789 mg, 1.98 mmol) in hexane (30 ml). A white precipitate instantaneously appeared and the reaction mixture became a yellow suspension. After stirring for 1 h, the mixture was filtered through a Celite pad and the precipitate was washed with hexane (15 ml × 3). The filtrate was concentrated to 5 ml under reduced pressure and was cooled to −40°C to give yellow crystals of **2b**. After removal of the mother liquor by a cannula, the crystals were washed with hexane (2 ml × 3) and then dried in vacuo. The second crop was obtained from a mixture of the mother liquor and washings in a similar manner. A total yield of **2b**: 730 mg (1.73 mmol, 87%). $^{13}C\{^1H\}$-NMR (75.5 MHz, C_6D_6): δ 0.9 (SiMe), 2.7 (SiMe), 9.8 (C_5Me_5), 22.7 (CH_3CO_2), 95.0 (C_5Me_5), 171.1 (CH_3CO_2), 217.7 (FeCO). Mass spectrum (EI, 70 eV): m/z 407 ($M^+ - Me$, 0.90), 352 (3.5), 320 (3.6), 305 ($M^+ - MeCO_2 - SiMe_2$, 5.7), 275 ($M^+ - MeCO_2 - SiMe_2 - 2Me$, 2.7), 247 ($Cp^*Fe(CO)_2^+$, 4.0), 175 ($M^+ - Cp^*Fe(CO)_2$, 100), 133 (17), 117 ($M^+ - Cp^*Fe(CO)_2 - SiMe_2$, 5.7), 73 (7.3). Anal. Found: C, 51.26; H, 7.12. Calc. for $C_{18}H_{30}FeO_4Si_2$: C, 51.18; H, 7.16%.

3.3. Synthesis of $Cp^*Fe(CO)_2SiMe_2SiMe_2O(2\text{-}C_5H_4N)$ (3)

Molecular sieves 4Å (1.9 g) and dry toluene (5 ml) were placed in a 50 ml Schlenk tube and Et_3N (0.3 ml) and 2-pyridone (97 mg, 1.02 mmol) were added to it. The mixture was stirred for 1 h and solid $Cp^*Fe(CO)_2SiMe_2SiMe_2Cl$ (**1b**) (401 mg, 1.01 mmol) was then slowly added. After stirring at room temperature for 1 h, a white precipitate was filtered off and was washed with toluene (1 ml × 3). The filtrate and washings were combined and the solvent was removed under reduced pressure. The residue was dissolved in 1 ml of dry pentane and cooled to −76°C. Yellow crystals of **3** were collected, washed with a small amount of pentane, and dried under reduced pressure. Yield of **3**: 199 mg (0.435 mmol, 43%). $^{13}C\{^1H\}$-NMR (75.5 MHz, C_6D_6): δ 1.7 (SiMe), 3.3 (SiMe), 10.0 (C_5Me_5), 95.1 (C_5Me_5), 112.9 (pyridine), 116.6 (pyridine), 138.8 (pyridine), 147.5 (pyridine), 163.4 (pyridine), 217.9 (FeCO). Mass spectrum (EI, 70 eV): m/z 457 (M^+, 0.03), 442 ($M^+ - Me$, 0.60), 429 ($M^+ - CO$, 0.50), 401 ($M^+ - 2CO$, 1.0), 210 ($M^+ - Cp^*Fe(CO)_2$, 100), 152 ($M^+ - Cp^*Fe(CO)_2SiMe_2$, 27). Anal. Found: C, 55.07; H, 6.85; N, 2.97. Calc. for $C_{21}H_{31}FeNO_3Si_2$: C, 55.13; H, 6.83; N, 3.06%.

3.4. Photolysis of $CpFe(CO)_2SiMe_2SiMe_2OCOMe$ (2a)

An H-shaped Pyrex glass tube (10 mm o.d.) connected to a ground glass joint through a Teflon needle valve was charged with **2a** (343 mg, 974 μmol) and was attached to a vacuum line. Hexane (6 ml) was introduced onto **2a** by a trap-to-trap-transfer technique and the Teflon needle valve was closed. The H-shaped tube was shut off from the vacuum line and was irradiated in a water bath kept at 5°C. Gas evolution was immediately observed and after 5 min a yellow powder began to precipitate. After irradiation for 20 min, the H-shaped tube was reattached to the vacuum line and the solution was degassed to remove the generated carbon monoxide. The solution was irradiated for a furthur 10 min and then degassed and flame-sealed under high vacuum. The reaction mixture was warmed to 60°C to

dissolve all the precipitate and was allowed to cool down to room temperature to give yellow crystals. After the mixture was concentrated to approximately 2 ml, the mother liquor was removed by decantation and the yellow crystals were washed with hexane (0.2 ml × 3) to give **4a** (187 mg, 577 μmol, 59%). $^{13}C\{^1H\}$-NMR (75.5 MHz, C_6D_6): δ 10.1 (SiMe), 11.8 (SiMe), 23.0 (CH_3CO_2), 78.4 (Cp), 183.4 (CH_3CO_2), 215.4 (FeCO). Mass spectrum (EI, 70 eV): m/z 324 (M^+, 100), 296 ($M^+ - CO$, 38), 281 ($M^+ - CO - Me$, 5.1), 266 ($M^+ - CO - 2Me$, 14), 253 ($M^+ - CO - MeCO$, 53), 236 ($M^+ - CO - 4Me$, 33), 195 (19), 175 ($M^+ - CpFe(CO)$, 31), 133 (13), 121 ($CpFe^+$, 40), 117 ($M^+ - CpFe(CO) - SiMe_2$, 16), 93 (24), 73 (38). Anal. Found: C, 44.51; H, 6.37. Calc. for $C_{12}H_{20}FeO_3Si_2$: C, 44.44; H, 6.22%.

3.5. Photolysis of Cp*Fe(CO)$_2$SiMe$_2$SiMe$_2$OCOMe (2b)

Photolysis of **2b** was carried out in a manner similar to that of **2a**. Irradiation of **2b** (402 mg, 952 μmol) in hexane (10 ml) at 10°C for 60 min in total afforded **4b** (279 mg, 707 μmol, 74%) as yellow columnar crystals. $^{13}C\{^1H\}$-NMR (75.5 MHz, C_6D_6): δ 8.6 (SiMe), 10.0 (SiMe), 11.0 (C_5Me_5), 22.9 (CH_3CO_2), 89.8 (C_5Me_5), 182.5 (CH_3CO_2), 216.7 (FeCO).). Mass spectrum (EI, 70 eV): m/z 394 (M^+, 100), 366 ($M^+ - CO$, 14), 336 ($M^+ - CO - 2Me$, 9.2), 322 (35), 320 ($M^+ - MeCO_2 - Me$, 54), 306 ($M^+ - CO - 4Me$, 11), 304 (13), 246 (43), 230 (18), 190 (44), 175 (36), 133 (51), 117 ($M^+ - Cp^*Fe(CO) - SiMe_2$, 19), 73 (30). Anal. Found: C, 51.82; H, 7.22. Calc. for $C_{17}H_{30}FeO_3Si_2$: C, 51.77; H, 7.67%.

3.6. Photolysis of Cp*Fe(CO)$_2$SiMe$_2$SiMe$_2$O(2-C$_5$H$_4$N) (3)

Photolysis of **3** was carried out in a manner similar to that of **2a**. Irradiation of **3** (135 mg, 295 μmol) in pentane (6 ml) at 5°C for 2 h in total afforded **5** (98 mg, 228 μmol, 77%) as yellow crystals. $^{13}C\{^1H\}$-NMR (75.5 MHz, toluene-d_8): δ 8.1 (SiMe), 9.1 (SiMe), 10.1 (SiMe), 10.5 (SiMe), 11.3 (C_5Me_5), 89.7 (C_5Me_5), 114.4 (pyridine), 118.7 (pyridine), 140.3 (pyridine), 142.7 (pyridine), 164.8 (pyridine), 217.7 (FeCO). Mass spectrum (EI, 70 eV): m/z 429 (M^+, 100), 442 ($M^+ - Me$, 0.60), 401 ($M^+ - CO$, 45), 399 ($M^+ - 2Me$, 56), 210 ($M^+ - Cp^*Fe(CO)$, 85), 152 ($M^+ - Cp^*Fe(CO)_2SiMe_2$, 47). Anal Found: C, 56.18; H, 7.40; N, 3.27. Calc. for $C_{20}H_{31}FeNO_2Si_2$: C, 55.93; H, 7.28; N, 3.26%.

3.7. X-ray crystal structure determination of 4a

A single crystal of **4a** was cut with a blade to the size suitable for X-ray structure analysis (0.40 × 0.35 × 0.35 mm) in a glove bag, and the crystal was mounted in a thin glass capillary and the capillary was flame-sealed. The intensity data were collected on a Rigaku AFC-6S four-circle diffractometer with graphite-monochromated Mo–K_α radiation at 20°C. Reflections (7585) with $3° < 2\theta < 55°$ were collected by an ω–2θ scan technique. Cell constants and an orientation matrix for data collection were determined from 25 reflections with 2θ angles in the range 22.1–24.8°. The reflection data were corrected for Lorentz and polarization effects. Absorption corrections were made by psi scan method. The crystal data and analytical conditions are listed in Table 2. The structure was solved by heavy-atom Patterson methods (DIRDIF-92 PATTY) [29] and refined by the block-diagonal least-squares method using individual anisotropic thermal parameters for all non-hydrogen atoms. All hydrogen atoms were placed at their geometrically calculated positions ($d_{CH} = 0.95$ Å) and refined with isotropic thermal parameters. The final R value was 0.049 and R_w was 0.073 aagainst the reflections for 2808 reflections with $I_o > 3\sigma(I_o)$. All calculations were performed using TEXAN crystallographic software package of Molecular Structure Corporation (1985 and 1992).

3.8. X-ray crystal structure determination of 5

Measurements were made on a Rigaku Raxis-Rapid Imaging Plate diffractrometer with graphite monochromated Mo–K_α radiation. Indexing was performed from two oscillations, which were exposed for 1.7 min. The camera radius was 127.40 mm. Readout was performed in the 0.100 mm pixel mode. The data were collected at a temperature of 20°C to a maximum 2θ value of 55.0. A total of 44 images, corresponding to 220 oscillation angles, were collected with 2 different goniometer settings. Exposure time was 0.5 min per degree. The structure was solved by Patterson and Fourier transform methods (SHELXS-97) [30]. All non-hydrogen atoms were refined by full -matrix least-squares techniques with anisotropic displacement parameters (SHELXL-97) [30]. All hydrogen atoms were placed at their geometrically calculated positions ($d^{CH} = 0.96$ Å for methyl hydrogen atoms and 0.93 Å for aromatic hydrogen atoms) and refined riding on the corresponding carbon atoms with isotropic thermal parameters ($U = 1.5\ U(C_{methyl})$ and $1.2U(C_{aromatic})$). The final R indices against the reflections with $I > 2\sigma(I)$ were $R_1 = 0.0496$ and $wR_2 = 0.1354$. The crystal data and analytical conditions are listed in Table 3.

4. Supplimentary material

Crystallographic data for the structural analysis has been deposited with the Cambridge Crystallographic Data Centre, CCDC no. 141145 for compound **4a** and

CCDC no. 141146 for compound **5**. Copies of this information may be obtained free of charge from the Director, CCDC, 12 Union Road, Cambridge CB2 1EZ, UK (Fax: +44-1223-336033; e-mail: deposit@ccdc.cam.ac.uk or www: http://www.ccdc.cam.ac.uk).

Acknowledgements

This work was supported by Grant-in-Aid for Scientific Research on Priority Areas (No. 09239105) from Ministry of Education, Science, Sports and Culture, Japan. We thank Dow Corning Toray Silicone Co., Ltd. and Shin-Etsu Chemical Co., Ltd., for a gift of silicon compounds.

References

[1] (a) M.D. Curtis, P.S. Epstein, Adv. Organomet. Chem. 19 (1981) 213. (b) B.J. Ayrett, Adv. Inorg. Chem. Radiochem. 25 (1982) 1. (c) T.D. Tilley, in: S. Patai, Z. Rappoport (Eds.), The Chemistry of Organic Silicon Compounds, Wiley, New York, 1989 (Chapter 24). (d) M.S. Eisen, in: Z. Rappoport, Y. Apeloig (Eds.), The Chemistry of Organic Silicon Compounds, vol. 2, Wiley, New York, 1998 (Chapter 35). (e) J.A. Reichl, D.H. Berry, Adv. Organomet. Chem. 43 (1999) 197.

[2] (a) K. Yamamoto, H. Okinoshima, M. Kumada, J. Organomet. Chem. 23 (1970) C7. (b) K. Yamamoto, H. Okinoshima, M. Kumada, J. Organomet. Chem. 27 (1971) C31. (c) I. Ojima, S. Inaba, T. Kogure, J. Organomet. Chem. 55 (1973) C7. (d) T. Sakakura, O. Kumberger, R.P. Tan, M.-P. Arthur, M. Tanaka, J. Chem. Soc. Chem. Commun. (1995) 193. (e) H. Yamashita, M. Tanaka, Bull. Chem. Soc. Jpn. 68 (1995) 403.

[3] (a) Y. Tanaka, H. Yamashita, M. Tanaka, Organometallics 14 (1995) 530. (b) K. Tamao, G.-R. Sun, A. Kawachi, J. Am. Chem. Soc. 117 (1995) 8043. (c) M. Okazaki, H. Tobita, H. Ogino, J. Chem. Soc. Dalton Trans. (1997) 3531.

[4] (a) J.A. Reichl, C.M. Popoff, L.A. Gallagher, E.E. Remsen, D.H. Berry, J. Am. Chem. Soc. 118 (1996) 9430. (b) S.M. Katz, J.A. Reichl, D.H. Berry, J. Am. Chem. Soc. 120 (1998) 9844.

[5] K.H. Pannell, J. Cervantes, C. Hernandez, J. Cassias, S. Vincenti, Organometallics 5 (1986) 1056.

[6] H. Tobita, K. Ueno, H. Ogino, Chem. Lett. (1986) 1777.

[7] (a) K. Ueno, H. Tobita, M. Shimoi, H. Ogino, J. Am. Chem. Soc. 110 (1988) 4092. (b) H. Tobita, K. Ueno, M. Shimoi, H. Ogino, J. Am. Chem. Soc. 112 (1990) 3415. (c) K. Ueno, S. Ito, K. Endo, H. Tobita, S. Inomata, H. Ogino, Organometallics 13 (1994) 3309.

[8] (a) H. Tobita, H. Wada, K. Ueno, H. Ogino, Organometallics 13 (1994) 2545. (b) H. Tobita, H. Kurita, H. Ogino, Organometallics 17 (1998) 2844.

[9] T. Takeuchi, H. Tobita, H. Ogino, Organometallics 10 (1991) 835.

[10] (a) K. Ueno, A. Masuko, H. Ogino, Organometallics 16 (1997) 5023. (b) K. Ueno, A. Masuko, H. Ogino, Organometallics 18 (1999) 2694.

[11] M. Okazaki, H. Tobita, H. Ogino, Chem. Lett. (1997) 437.

[12] H. Tobita, H. Kurita, H. Ogino, Organometallics 17 (1998) 2850.

[13] K. Ueno, K. Nakano, H. Ogino, Chem. Lett. (1996) 459.

[14] K. Ueno, M. Sakai, H. Ogino, Organometallics 17 (1998) 2138.

[15] K. Ueno, K. Yamaguchi, H. Ogino, Organometallics 18 (1999) 4468.

[16] H.K. Sharma, K.H. Pannell, Chem. Rev. 95 (1995) 1351.

[17] (a) D.C. Pestana, T.S. Koloski, D.H. Berry, Organometallics 13 (1994) 4173. (b) L.K. Figge, P.J. Carroll, D.H. Berry, Organometallics 15 (1996) 209.

[18] U. Bodensieck, P. Braunstein, W. Deck, T. Faure, M. Knorr, C. Stern, Angew. Chem. Int. Ed. Engl. 33 (1994) 2440.

[19] (a) G.P. Mitchell, T.D. Tilley, G.P.A. Yap, A.L. Rheingold, Organometallics 14 (1995) 5472. (b) G.P. Mitchell, T.D. Tilley, Organometallics 15 (1996) 3477.

[20] S. Nlate, E. Herdtweck, R.A. Fischer, Angew. Chem. Int. Ed. Engl. 35 (1996) 1861.

[21] (a) H. Tobita, H. Ogino, J. Synth. Org. Chem. Jpn. 53 (1995) 530. (b) H. Tobita, H. Ogino, Bull. Chem. Soc. Jpn., in preparation

[22] H. Wada, H. Tobita, H. Ogino, Organometallics 16 (1997) 2200 and references cited therein.

[23] Y. Etienne, C.R. Acad. Sci. Paris 235 (1952) 966.

[24] K. Nakamoto, Infrared and Raman Spectra of Inorganic and Coordination Compounds, 4, Wiley, New York, 1986.

[25] H. Kobayashi, K. Ueno, H. Ogino, Chem. Lett. (1999) 239.

[26] A.G. Orpen, L. Brammer, F.H. Allen, O. Kennard, D.G. Watson, R. Taylor, J. Chem. Soc. Dalton Trans. (1989) S1.

[27] (a) J.R. Koe, H. Tobita, T. Suzuki, H. Ogino, Organometallics 11 (1992) 150. (b) J.R. Koe, H. Tobita, T. Suzuki, H. Ogino, Organometallics 11 (1992) 2479.

[28] H. Wada, H. Tobita, H. Ogino, Chem. Lett. (1998) 993.

[29] PATTY: P.T. Beurskens, G. Admiraal, G. Beurskens, W.P. Bosman, S. Garcia-Granda, R.O. Gould, J.M.M. Smits, C. Smykalla, The DIRDIF program system, Technical Report of the Crystallography Laboratory, University of Nijimegen, The Netherlands, 1992.

[30] G.M. Sheldrick, SHELX-97: Program for Crystal Structure Determination, University of Göttingen, Germany, 1997.